PROCEEDINGS OF SPIE

SPIEDigitalLibrary.org/conference-proceedings-of-spie

Review of the development of 2k2 IR FPAs for astronomy and Space in Europe

G. Badano, C. Cervera, O. Gravrand, B. Fièque, A. Lamoure, et al.

G. Badano, C. Cervera, O. Gravrand, B. Fièque, A. Lamoure, O. Boulade, S. Mouzali, "Review of the development of 2k2 IR FPAs for astronomy and Space in Europe," Proc. SPIE 10766, Infrared Sensors, Devices, and Applications VIII, 107660H (18 September 2018); doi: 10.1117/12.2323496

SPIE.

Event: SPIE Optical Engineering + Applications, 2018, San Diego, California, United States

Review of the development of 2k2 IR FPAs for astronomy and space in Europe

G. Badano (a), C. Cervera (a) O. Gravrand (a), B. Fièque (b) , A. Lamoure (b) , O. Boulade (c), S. Mouzali (c)

(a) Univ. Grenoble Alpes, CEA LETI MINATEC, 17 rue des Martyrs Grenoble and Univ. Grenoble Alpes, F-38000 Grenoble, France
(b) Sofradir, 364 route de Valence, 38113 Veurey-Voroize, FRANCE
(c) CEA, Institut de Recherche sur les Lois Fondamentales de l'Univers, Service d'Astrophysique, Orme des Merisiers, 91191 Gif-sur-Yvette, France

ABSTRACT

We report on the development of short wave infrared (SWIR) imaging arrays for astronomy and space observation in Europe. LETI and Sofradir demonstrated 640x480 SWIR HgCdTe (MCT) arrays geared at low flux, low dark noise operation. Currently, we are developing 2048x2048 arrays mated to a newly developed ROIC. In parallel, the European Space Agency and the European Commission are funding the development and industrialization of 4'' CdZnTe substrates and HgCdTe epitaxy. These large wafers are needed to achieve the necessary economies of scale and address the need for even larger arrays. HgCdTe SWIR detector performance at LETI/Sofradir is known from previous programs and will be discussed here. However, we will only be able to summarize the features and specifications of the new 2048x2048 detectors which are still at a prototype stage.

Keywords: Infrared detection, astronomy, SWIR

* Corresponding author**,** E-mail: giacomo.badano@cea.fr

1. INTRODUCTION

Detectors used in astrophysics aim at sensing very low photon fluxes, to image stars and perform high-resolution spectrometry. Increasing the FPA size while reducing dark and readout noise have been the themes of IR focal plane array (FPA) development in recent years. The only materials that achieve the current noise specifications are InSb and HgCdTe, the former with a cutoff wavelength of 5.2 µm. For SWIR operation, HgCdTe is the material of choice because its gap can be tuned to the proper wavelength range.

Since the 2010's the European Space Agency (ESA) has established a European roadmap to produce a low flux, low noise IR FPAs for astronomy called NIRLFSA (from Near Infrared Low Flux Spectral Array) now rechristened ALFA (Astronomy Large Focal plane Array). During that program, detector size has increased from 384x288 pixels of the first prototypes [1] to 640x480 [2], to the upcoming 2048x2048 pixels. The first two generations of detectors explored the ultimate performance of HgCdTe FPAs in terms of dark current, readout noise and quantum efficiency (QE). The current third generation, now in an advanced phase of definition and fabrication, consists of 2048x2048 pixel detectors with a suitable source follower input stage (SFD) ROIC. These new detectors, born out of a collaboration of LETI and Sofradir, are based on a p-on-n HgCdTe technology, 15 µm pitch.

Infrared Sensors, Devices, and Applications VIII, edited by Paul D. LeVan, Priyalal Wijewarnasuriya, Arvind I. D'Souza, Proc. of SPIE Vol. 10766, 107660H · © 2018 SPIE
CCC code: 0277-786X/18/$18 · doi: 10.1117/12.2323496

2. DEVICE AND ROIC DEVELOPMENT

The principal figures of merit for astronomical applications are the QE and the total noise. The dark noise depends on the diode structure whereas the readout noise comes mainly from the ROIC input stage. In HgCdTe SWIR photodiodes at low temperatures (typically below 150K for n-type material), the dark noise is mainly due to trap-assisted generation-recombination (GR) in the space charge region of the device. An electron hole pair is created within a minority carrier diffusion length of the junction. One of the two carriers is then trapped by a defect and the other is collected by the diode, if its lifetime is longer than the integration time. At higher temperatures, the dark current is dominated by random thermal generation of electron hole pairs in the bulk which diffuse into the junction. Both the carrier diffusion length and the width of the space charge region under bias are affected by the doping level, which must be optimized. Also, to reduce GR noise, one needs to minimize the density of trapping centers, hence the defect density both in the bulk and on the surface.

Sofradir legacy technology relies on p-type vacancy doped absorbing material. As it happens, extrinsic doping achieved during growth is preferable to vacancy doping, because vacancies are point defects that generate dark noise. Hence, p-on-n diodes doped with In during growth were explored in the recent phases of NIRLFSA. In those diodes, depicted in Figure 1, the junction is formed by As implantation followed by two annealing steps, to heal implantation defects and activate the dopant, while filling Hg vacancies to restore the In doping level. Carriers are photogenerated everywhere in the MCT volume and are collected by diffusion to the junction. Such planar geometry maximizes the QE. While legacy n-on-p, vacancy doped layers were also studied to get a baseline dark current value, all recent developments rely on p-on-n diodes to cope with specifications.

The impact of the material growth technique on GR was explored first. The NIRLFSA detectors were grown either by liquid phase (LPE) or molecular beam epitaxy (MBE) on perfectly lattice matched CdZnTe substrates. A wide gap surface passivation layer can be easily deposited *in situ* during MBE growth, but it must be deposited after growth on LPE wafers. Another difference is that the dislocation density is higher for MBE than LPE. At any rate, we observed that whatever the effect of the growth technique on the dark current at the operating temperature of 100K, it was overshadowed by that of the doping level [3], which is probably responsible for the different diode capacitance (16 fF for LPE and 10 fF for MBE).

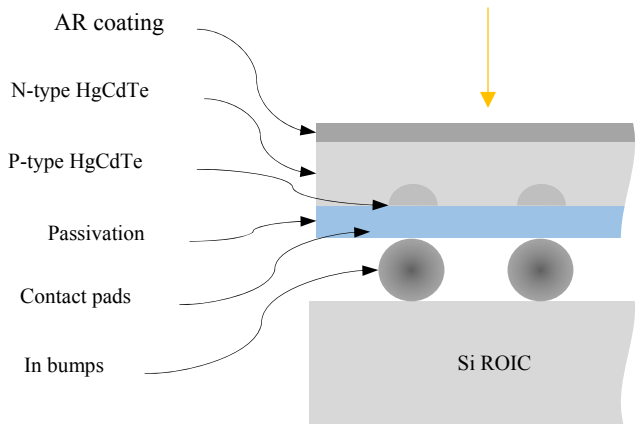

Figure 1. SWIR HgCdTe detector architecture

Another crucial choice is the ROIC design scheme. The efficiency of direct injection ROIC input stages is too small for low flux detectors. The other two common options are capacitive trans-impedance amplifier (CTIA) and source-follower (SFD). CTIA provides a constant bias while the pixel is read, but is more prone to producing glow and bring in additional noise due to the numerous electronic components. Source follower SFD designs, whereby the

integration is carried out on the diode capacitance itself, are preferred in the astronomy community because they minimize power consumption, electronic noise and glow. The current small-format 640x480 pixel ROICs have been developed since 2010. They show a very low readout noise of about 7e- rms (single readout) for a readout rate of typically 100kpixel/s. At the operating bias voltage chosen for measurements, the non-linearity is typically 3% over a 60ke- dynamic range. The upcoming 2k² ALFA ROIC is poised to replicate these results.

The readout electronic noise is determined by the interplay between the diodes and the readout circuit. During integration, the photogenerated carriers charge the diode intrinsic capacitance, until they are let to flow into another capacitance embedded in the ROIC. The total integration capacitance is the sum of the diode and the ROIC node capacitances. It determines the charge to voltage conversion gain and plays a key role in shaping the readout noise. The diode full well capacitance is proportional to the doping level, which as we mentioned, also impacts the diffusion length, the dark current and the quantum efficiency. A tradeoff doping level was chosen during the first two generations of NIRLFSA detectors to maintain the QE and minimize the dark current.

Figure 2 [4] summarizes the dark current results obtained from the first two generations of NIRLFSA detectors. The detectors vary in size, cutoff wavelength (1.96 µm to 2.12 µm) and material fabrication method. The pixel pitch is 15 µm. The cutoff wavelength is comprised between 1.96 and 2.5 µm measured at 80K. Due to the planar diode design, the QE reaches 70% without antireflection (AR) coating and 90% with AR coating. The dark current follows the expected diffusion trend at temperatures above 150K, then it saturates at 0.1e-/pixel/s independently of the material growth method, cutoff and diode structure. Note that the first two MBE-grown layers had a higher doping level than the other layers, resulting in excess noise in the diffusion regime.

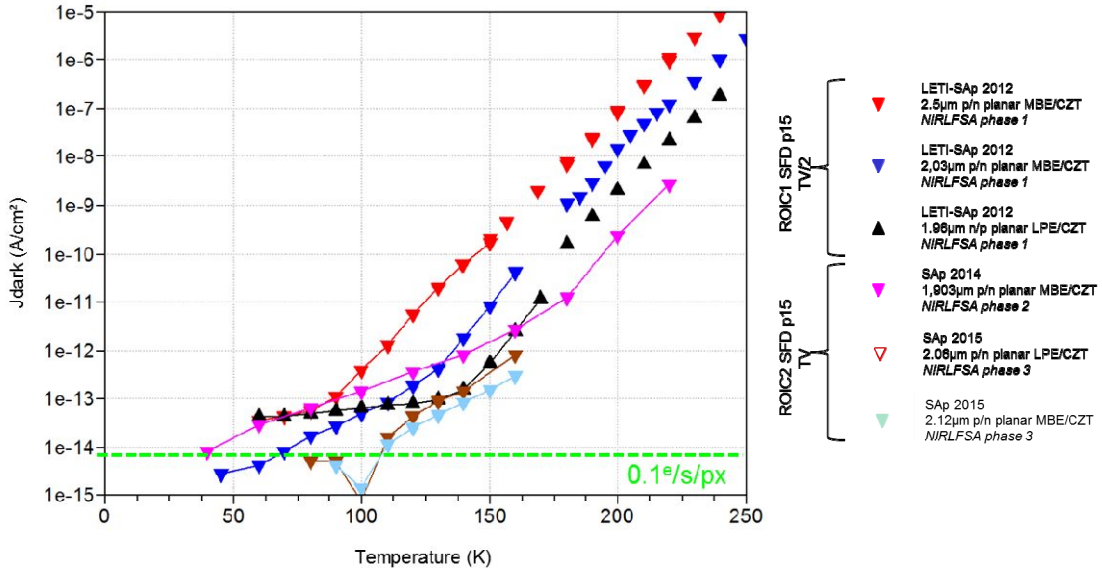

Figure 2. Dark current levels for phase 1 and 2 detectors of the European NIRLFSA program, reproduced from reference 4. The points at and below 100K for phase 2 detectors were obtained by extrapolation as explained in the text.

The dark current map for the MBE and LPE detectors are shown in the Figure 3 for a 100K operating temperature. The map shows that the dark current is dominated by ROIC glow at a level of 10 to 20 e-/s/pixel. To show that the

origin of the excess noise is indeed the glow, the ROIC was operated in such a way as to halve the video output current. That resulted in halving the noise. A tentative extrapolation of the dark current level without glow was possible (it was supposed that the dark current measured at 60K was entirely due to glow). That led to an estimation of < 0.5e/s/pixel, most likely 0.1 e-/s/pixel [2] [3] for the LPE grown devices. However, to date, no actual, accurate dark current measurement at 100K is available. As it happens, the best Hawaii 2rg detectors exhibit dark currents of the order of 0.02 e-/s/pixel [5].

The dynamic range is affected by the use of an SFD ROIC that is by nature nonlinear. The range of linearity depends on the interplay of the diode and the ROIC capacitance. The diode capacitance is around 15-20 fF at a 400 mV bias and the ROIC capacitance was 4 fF. Nonlinearity is less that 3% at a 60 ke- output level [3].

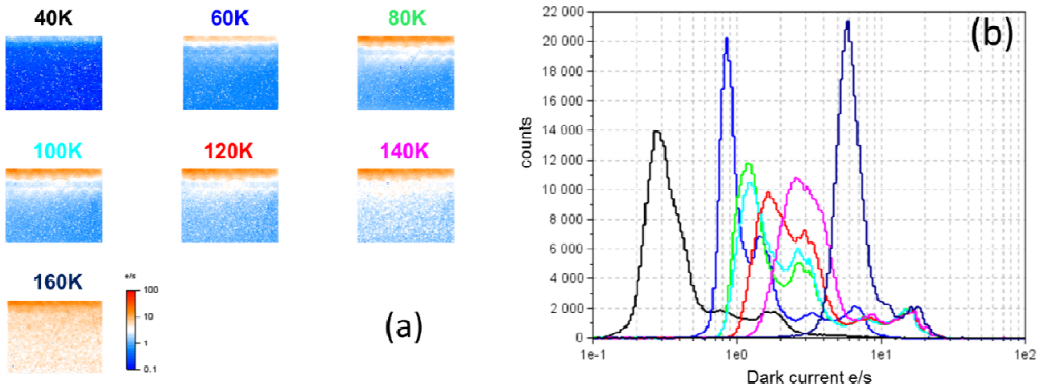

Figure 3 (from reference [2]). (a) signal distribution across a 640x512 pixel SWIR array, showing a current gradient that suggests glow (b) Distribution of the dark currents at the different temperatures. The excess noise population corresponds to the top rows of the images in (a).

The NIRLFSA detectors were recently subjected to proton and gamma irradiation [6]. The substrate of the irradiated detectors was entirely removed to avoid proton induced luminescence. The authors report a 24% increase in the dark current upon irradiation of a dose equivalent to 5 times the end life of the detector at the Lagrange L2 point. The number of pixels affected by a dark current increase > 5e-/s/pixel was of 6%. That is deemed acceptable for most astrophysics missions. The dark current increased by 24%. Gamma irradiation occurred according to a standard protocol from 10 krad up to 50 krad, using a flux of 2 krad/hour. As the authors of the study show, the areas of the detectors that had previously been exposed to proton irradiation are not affected by the gamma radiation. Gamma irradiation tests performed on an MCT NIR Hawaii-2rg detector from Teledyne [7] showed an increase of dark current by a factor up to 56%, consistent with the results of [6]. The NIRLFSA detectors have also been tested for persistence [8] along with the Hawaii 2rg detectors [6] [8]. Both the Hawaii 2rg and the NIRLFSA detector persistence saturate above full well. Therefore, it seems likely that both bulk and surface traps come into play. Interestingly, irradiation decreases the NIRLFSA persistence by 15%. That is due to the filling of electrically active traps. Decreasing persistence further can be accomplished by reducing the potential difference across the passivation layer (Figure 1) and perfecting material quality to decrease the bulk trap density. We are currently working at some of these issues.

3. ALFA DETECTORS AND ROIC.

The aim of this third installment of the NIRLFSA program is to replicate the characteristics of the smaller arrays above on a much larger format. Chief among those, the dark noise and the QE. That entails a device fabrication and a material fabrication effort. The specifications and diode design are nearly identical to that of past NIRLFSA

projects (Table 1), but the ROIC was redesigned from scratch. The principal specifications of the new detector ROIC are given in the Table 2. The ALFA readout circuit size is approximately 3x3 cm², requiring stitching. Its architecture is portrayed in Figure 4, in green the analog and in blue the digital parts. Data are provided via 32 outputs, plus a reference output linked to a reference pixel that is disconnected from the photodiode array. According to ESA's demand, there are 4 operating modes detailed in Table 2; they are (i) a rolling shutter mode, with a readout frequency up to 100 kHz, which guarantees low readout noise and power consumption, for scientific applications (ii) a fast mode, up to 6 MHz (iii) a windowed mode, useful to define 3 refreshed windows per output channel and (iv) tracking mode which interlaces a window readout and a full science mode readout of the whole array. The array can be reset either globally, or line by line, or pixel by pixel. One can also keep a certain amount of pixels under permanent reset while others integrate the incoming flux. That makes it easier to measure, for instance, the interpixel capacitance.

Table 1. Specifications of the ALFA detectors

Parameter	Value
Array size - pitch	2048x2048 – 15µm
Spectral range	Cut-on ≤ 0.8µm, cut-off 2.1µm / 2.5µm
Operating temperature	100 ± 1 K
Quantum efficiency	≥ 70%
Dark current (at 100K)	≤ 0.1 e-/pix/s
Linear well capacity	≥ 60ke-
Non linearity	≤ 3%
Cross talk : inter pixel capacitance / other contributions	≤ 2% / ≤ 3%
Readout noise (single CDS)	≤ 18e- rms
Readout speed	≥ 100kHz

Power consumption is an essential parameter for many space born scientific applications. Table 3 gives it as function of the number of outputs under default (science) operating conditions. In fast mode, the power consumption increases substantially. The charge handling capacity (CHC), linearity and noise levels were calculated from a simulation of the ROIC, corroborated by data obtained on smaller NIRLFSA arrays. The CHC of the ROIC is 135 ke. The rms readout noise is 30 µV, split in equal parts between source follower input stage noise and output stage noise. That equals 11e- approximately.

Hybridizing such a large array to the ROIC has many challenging aspects. The surface topology (contact, passivation) must be very accurately controlled together with the substrate flatness. A specific chemical-mechanical polishing technique has been developed to minimize the surface roughness.

The crosstalk is mainly driven by intrapixel capacitance, i.e. parasitic capacitance that builds up between adjacent diodes. The IPC readout mode has been proposed to measure that capacitance. Based on previous NIRLFSA measurements, the IPC will be <3%.

Table 2. ROIC main features.

	Science mode	Fast mode	Windows mode	Tracking mode
Number of pixels read	2048x2048	2048x2048	Up to 3 windows defined by SerDat	Up to 3 windows defined by SerDat
Readout	Rolling shutter			
Reset mode	Line by line, pixel by pixel, global reset, single pixel restet			
Pixel readout frequency	Up to 100 kHz	Up to 6 MHz	100 kHz	100 kHz
Number of outputs	1, 4 or 32	32	1, 4, 32	1,4, 32
Full frame time with 32 outputs	1.43s	0.024 s	Depents on window size	Depents on window size
Analog chain	Slow	Fast	Slow	Slow
Comment	Low noise and weak consumption	Sample and hold in the column ouput amplifier	1, 2 or 3 windows per output	The science and window data are interlaced

Table 3. ROIC simulated power consumption.

	1 output	4 outputs	32 outputs
Current	0.18 mA	0.25 mA	0.85 mA
Power	0.6 mW	0.82 mW	2.8 mW

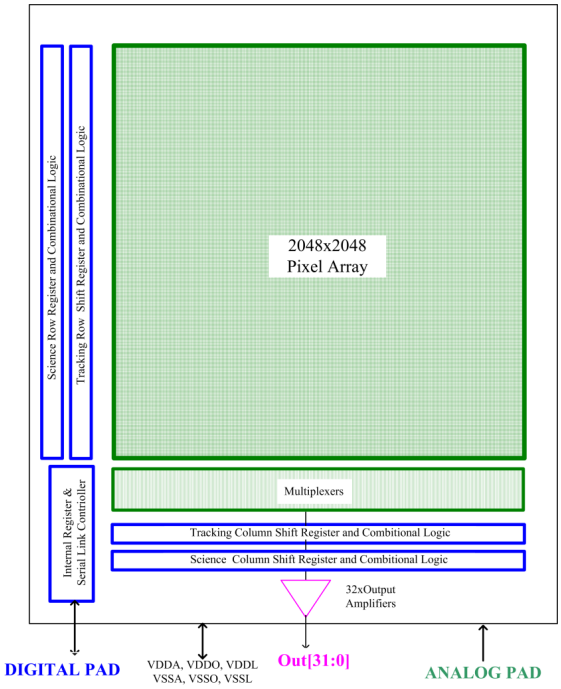

Figure 4. Architecture of the ALFA ROIC.

4. LARGE AREA FPA MANUFACTURING

In parallel with the design and fabrication of the detectors, LETI and Sofradir are involved since 2017 in a 3-year effort called Asteroid to industrialize the fabrication of SWIR FPAs. The first goal of Asteroid is to develop the pull of large area CdZnTe ingots. From these, substrates of sizes up to 4'' are obtained by dicing and polishing. A single 4'' substrate can house four 2k² FPAs, with sizable economies of scale. The preferred substrate orientation is (111)B and the Zn composition to obtain lattice matching with the epilayer is approximately 2%.

The growth technique of choice for HgCdTe epilayers at Sofradir is liquid phase epitaxy (LPE). The development of large area epitaxy for large volume production was carried out in tandem at LETI and Sofradir. The first 7x7 cm² epilayers were demonstrated very recently (Figures 6 and 7). Chemical mechanical double side polishing is being perfected to achieve a surface flat enough for hybridization, to increase yields. While the epilayer crystalline perfection, measured by the full width at half maximum of the X-ray rocking curve, is state of the art (50 arcsec), the surface morphology (depicted in Figure 7) is still degraded by the presence of a few macrodefects and other imperfections, which will require further substrate development. Finally, a complete 2k² manufacturing line compatible with 4'' sizes is envisioned.

The Asteroid program brings on board partners from across Europe: LETI and Sofradir, but also EVG, SME ADDL and IFAE. EV Group (EVG) is a leading supplier of equipment and process solutions for the manufacture of semiconductors, microelectromechanical systems (MEMS), compound semiconductors, power devices, and nanotechnology devices. Key products include wafer bonding, thin-wafer processing, lithography/nanoimprint lithography (NIL) and metrology equipment, as well as photoresist coaters, cleaners and inspection systems. The Spanish research institute IFAE is specialized in detector testing and has contributed to CERN detectors (ATLAS, ALEPH and several R&D projects), Neutrino physics (T2K), in Gamma-Ray astrophysics (MAGIC, CTA) and

Cosmology (DES, DESI, PAU, Euclid). Finally, SME ADDL will bring its experience in advanced modeling using finite element software.

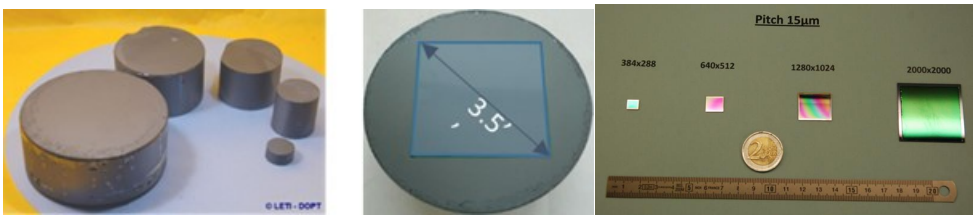

Figure 5 CZT Ingot size increase @CEA LETI

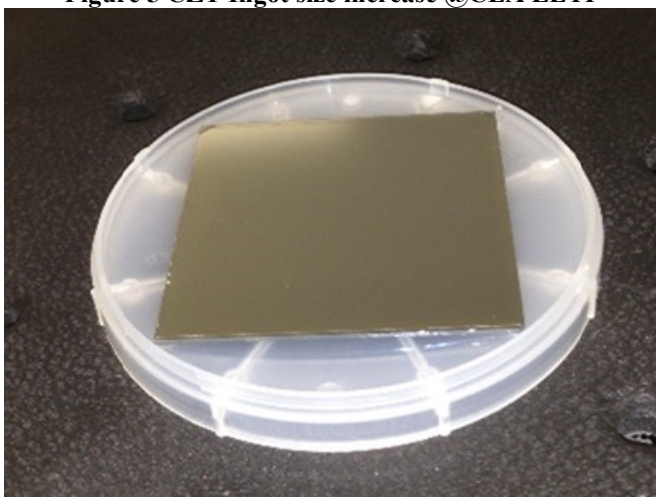

Figure 6 First epilayer of $Hg_{0,52}Cd_{0,48}Te$ onto $Cd_{1-y}Zn_yTe$ with a 72 x 73 mm² format @CEA LETI

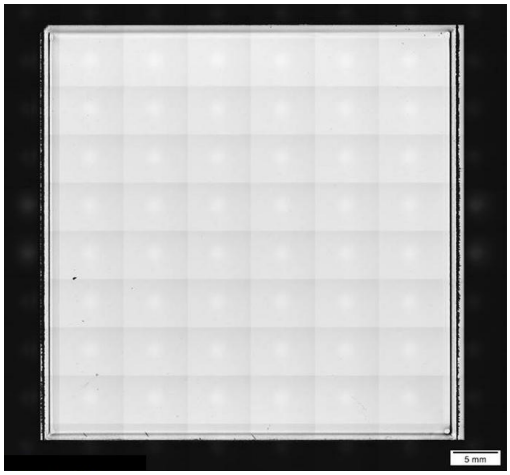

Figure 7. 72*73 mm² CZT with CMT epitaxy – rebuilt picture obtained by stitching optical microscopy

5. CONCLUSIONS

European institutional funding has fostered the development of low dark noise, low flux focal plane arrays at LETI and Sofradir since 2010. There is indication that HgCdTe technology based on extrinsic LPE material is capable to achieve the very stringent dark noise requirements, but the accuracy of dark noise measurements was reduced by ROIC glow. The array size has steadily increased over the years. Since 2016, large area 2048x2048, 15 µm pitch FPAs and glow free ROICs are being developed based on previous experience, to achieve industrialization on a three year horizon.

REFERENCES

[1] O. Gravrand, L. Mollard, O. Boulade, V. Moreau, E. Sanson, & G. Destefanis, Ultralow-Dark-Current CdHgTe FPAs in the SWIR Range at CEA and Sofradir. Journal of Electronic Materials, 41(10) (2012), 2686–2693. Doi:10.1007/s11664-012-2181-8

[2] C. Cervera, O. Boulade, O. Gravrand, C. Lobre, F. Guellec, E. Sanson, P. Ballet et al. "Ultra-low dark current HgCdTe detector in SWIR for space applications." Journal of Electronic Materials 46, no. 10 (2017): 6142-6149.

[3] O. Boulade, V. Moreau, P. Mulet, O. Gravrand, C. Cervera, JP. Zanatta, and J. Roumegoux, "Development activities on NIR large format MCT detectors for astrophysics and space science at CEA and SOFRADIR. In High Energy, Optical, and Infrared Detectors for Astronomy VII (Vol. 9915, p. 99150C). International Society for Optics and Photonics (2016).

[4] H. Geoffray, O. Boulade, B. Fièque, O. Gravrand, J. Rothmann, J. P. Zanatta, L. Tauzième, and A. Bardoux. "CNES detector development for scientific space missions: status and roadmap for infrared detectors." In High Energy, Optical, and Infrared Detectors for Astronomy VI, vol. 9154, p. 915402. International Society for Optics and Photonics.

[5] G. Finger, I. Baker, M. Downing, D. Alvarez, D. Ives, L. Mehrgan, M. Meyer, J. Stegmeier, and H. J. Weller. "Development of HgCdTe large format MBE arrays and noise-free high speed MOVPE EAPD arrays for ground based NIR astronomy." In International Conference on Space Optics—ICSO 2014, vol. 10563, p. 1056311. International Society for Optics and Photonics, 2017.

[6] P-E Crouzet, S.Tetaud, D.Gooding, B.Shortt, T. Beaufort, S.Blommaert, B. Butler, G. Van Duinkerken, J. ter Haar , F.Lemmel, K. van der Luijt, H. Smit, "First Proton and Gamma Radiation of the MCT NIR European Astronomy Large Format Array Detector", presented at the IEEE Nuclear and Space Radiations Effects Conference, Hawaii, USA, 2018.

[7] Penny Warren "Total ionizing dose response of the Hawaii-2RG focal plane array", Proc. SPIE 5902, Focal Plane Arrays for Space Telescopes II, 59020N, 25 August 2005

[8] P.E. Crouzet, "ESA activities for the ALFA – Astronomy Large Format Arrays – activity", presented at"Near IR large format focal plane arrays for scientific applications" Marseille, France, 2017